A 80-KW ISOLATED DC–DC CONVERTER FOR RAILWAY APPLICATIONS

A.Harish [1] M.Bharathi[2] E.Vejetha Dr.M.Ramesh
[12]Student of B.Tech(EEE) Assistant Professor of EEE Professor & HOD of EEE
vejethaerugurala@gmail.com marpuramesh223@gmail.com
Vaageswari College Of Engineering,Karimnagar

Abstract—This paper provides an analysis of a three-phase dual active bridge (DAB) topology used as high-power-density dc–dc converter for railway applications. The three-phase DAB is analyzed concerning the current intervals, the output power, and soft switching region, including the impact of zero-voltage switching capacitors. Furthermore, two measures are proposed to achieve soft-switching in the entire operating range, being auxiliary inductors and a straightforward switching strategy called the burst mode. Optimal component values are calculated to minimize losses in the complete operating range and to assess which measure is best suited. A prototype with the specifications acquired from the application has been built, yielding an efficiency of 95.6% at a nominal output power of 80 kW.

Index Terms—DC–DC power conversion, power electronics, power supplies, rail transportation electronics.

I. INTRODUCTION

Since the electrification of rail transportation systems, the amount of additional electrical systems in the vehicle has been increasing substantially. These, so called “auxiliary systems” are all systems on a rail vehicle that have functions other than traction. Nowadays, many auxiliary systems are present on rail vehicles. Examples are lighting, compressors, pumps, air-conditioning, and passenger information systems. In order to provide energy to these auxiliary systems, an auxiliary power unit (APU) converts the voltage from the overhead line or a third rail to the required levels of supply voltages. The total auxiliary power demand is typically in the range of tens of kilowatts up to a few hundreds of kilowatts. For safety reasons, galvanic isolation between the input and the output of the APU is required. In conventional APUs, the galvanic isolation is often realized with low-frequency transformers, an example is shown in Fig. 1(a). These transformers are bulky and result in relatively large and heavy APUs. Especially for light rail vehicles, like trams and metros, this becomes a problem when the auxiliary power demand increases. Therefore, size and weight reduction of the APU is necessary to meet the auxiliary power demand within the capabilities of light rail vehicles.

Most of the light rail transport systems are using a dc electrification system with common nominal voltages of 600 or 750V.

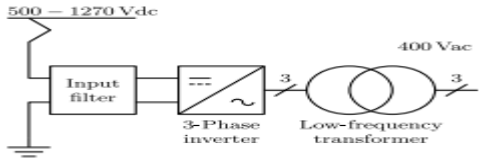

(a)

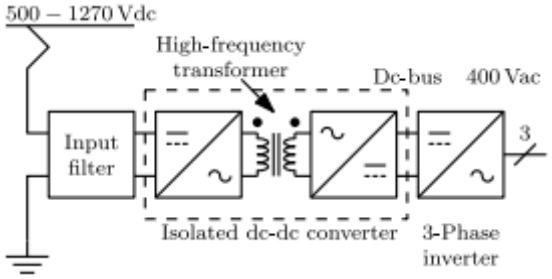

(b)

Fig:1. Simplified schematic of an APU. (a) Conventional APU. (b) Proposed APU.

TABLE I

REQUIREMENTS FOR THE INVESTIGATED DC–DC CONVERTER

Requirement	Value
Input voltage range	500–900 V
Peak input voltage	1270 V
Output voltage	600V
Continuous output power	80 kW
Switching frequency	20 kHz

Adding an isolated dc–dc converter is the preferable solution for reducing size and weight of the APU. By placing the isolated dc–dc converter between the input filter and the three-phase inverter, the bulky low-frequency transformer can be omitted, as can be seen in Fig. 1(b). This paper focuses on the design of an isolated dc–dc converter for railway applications. The requirements for the investigated dc–dc converter are presented in Table I. In Section II, the results of several publications concerning power density, soft-switching techniques, and comparison of different topologies are discussed.

II. TOPOLOGY OVERVIEW

The field of high-power-density dc–dc converters has been addressed often in the last decades. From the beginning, the conventional full-bridge converter topology has been the preferred choice to realize a high-power dc–dc converter [1]. However, due to problems with the leakage inductance of the transformer and, consequently, reverse recovery losses of the output diodes, the maximum switching frequency is limited. To solve this problem, several solutions were presented, including active clamps and/or auxiliary circuits [2]–[4]. These solutions enable higher switching frequencies at the expense of additional components and could lead to higher device stress. The

additional components impede the increase in power density and increased complexity, while the efficiency is often not better compared to other zero-voltage switching (ZVS) and zero-current switching (ZCS) techniques.

Resonant converter topologies offer possibilities for ZVS or ZCS, enabling high efficiencies and power densities [5]–[7]. The series resonant or LLC converter provides a load independent operating point with unity voltage gain at a switching frequency near the resonance frequency [6], [8]–[10]. However, this load independent operating point is lost when the input and/or output voltage changes, and switching frequency control is necessary to regulate the output voltage. Therefore, a boost converter can be used to regulate the input voltage in order to guarantee operation in the load independent operating point. Alternatively, the resonance circuit can be influenced by a switch-controlled capacitor, resulting in fixed frequency operation. Despite the provided solutions, the LLC converter still suffers from high rms phase currents, requiring a relatively large series resonant capacitor that leads to a decreased power density. The additional boost converter or switch-controlled capacitor also deteriorates the power density and efficiency.

The dual active bridge (DAB) topology introduced in [1] is an attractive alternative to the problems with the classical full-bridge topology. In comparison with the conventional full bridge topology, the output inductor is transferred to the ac side, and is in series with the leakage inductance. Consequently, the energy in the leakage inductance is transferred to the load without causing reverse recovery losses in the output diodes. This allows higher switching frequencies and, therefore, an increase in power density. Furthermore, the use of an active output bridge also increases the power density of the transformer [1]. When the desired inductance can be incorporated in the transformer, again the power density can be increased. In, very high power densities, up to 11.13kW/ L, are reported.

A three-phase DAB, also proposed in [1], has some advantages in comparison to the single-phase DAB. The three-phase DAB has lower turn-off currents in the switches and lower rms currents per phase. Also, the VA ratings for the input and output filters are significantly lower and can even go to zero due to the three-phase characteristics. Besides the lower VA ratings, the effective ripple frequency of the filter currents is three times higher, allowin g to use smaller filters. Compared to the single-phase DAB, the currents through the transformer windings are much more sinusoidal, resulting in reduced high frequency losses in the transformers [14]. A comprehensive comparison of single-phase and three-phase DAB topologies is given.

Both the single-phase and three-phase DAB topologies suffer from a limited soft-switching range in case the input voltage and the reflected output voltage are not equal. For the single-phase DAB, there exist switching strategies or modulation schemes for increasing the soft-switching range. These are described in [16]– [20]. Here, the soft-switching operating range is increased and also the overall efficiency can be increased with a minimum loss modulation strategy. The three-phase DAB does not possess these advantageous switching possibilities. The phase shift angle φ between the bridge voltage is the only control variable as the symmetrical properties of the three-phase system have to be maintained.

Although the three-phase DAB has less switching possibilities, compared to the single-phase DAB, and includes four extra switches, the topology has the most preferred properties for designing a high-power density isolated dc–dc converter. It has the lowest component ratings and is capable of achieving higher output powers with possibly the highest power density. For APU applications in light rail vehicles, high-power capability and power density are decisive. Therefore, the three-phase DAB topology is selected in this study.

III. THREE-PHASE DAB DC–DC CONVERTER

The three-phase DAB, shown in Fig. 2(a), consists of two three-phase bridges coupled with a three-phase transformer connected in Y–Y. The bridges are operated in six-step mode at a constant frequency. By applying a phase shift between the input and Output Bridge, the power flow can be controlled. Because the converter is symmetrical from input to output, bidirectional power flow is possible. The transformer leakage inductances are used as current transfer elements and, therefore, not considered as parasitic. If the magnetizing inductance Lm is neglected, an equivalent circuit can be used for analysis. In this circuit, only the total leakage inductance Ls seen from the primary side is connected between the phase legs from the input and output bridge. The corresponding idealized waveforms are shown in Fig. 2(b).

A. Analysis

To analyze the soft-switching region, the current of phase A is defined for the first six intervals as depicted in Fig. 2(b). The current iA in the different intervals is given in (3) for phase shifts of $0 \leq \varphi \leq \pi 3$. For phase shifts of $\pi 3 \leq \varphi \leq 2\pi 3$, a second set of equations, not given here, is utilized for further analysis of the soft-switching region. The magnetizing inductance Lm of the transformer is neglected in the analysis.

Furthermore, the angular frequency is defined as $\omega = 2\pi fs$, with fs the switching frequency in Hertz. The transformer's leakage inductance is indicated with Ls and the input and output voltage are defined as Vi and Vo , respectively. The reflected output voltage is given by $V o = VoN$, with N the turns ratio of the transformer.

Because the phase current is symmetric, the current iA (0) can be found by solving the set of equations, assuming steady-state

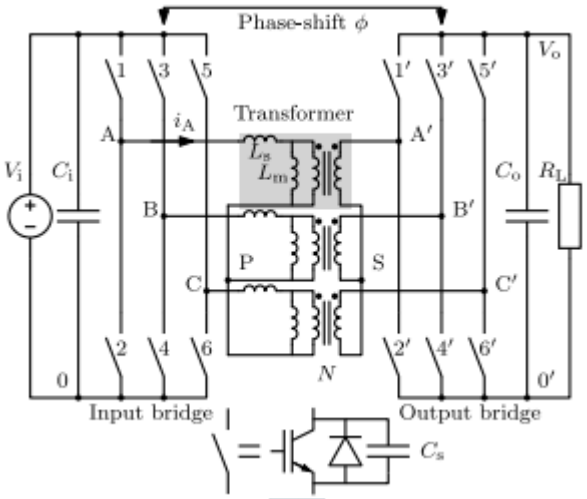

(a)

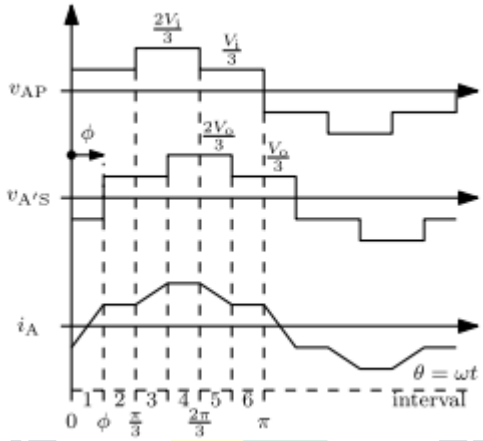

(b)

Fig. 2. Three-phase DAB. (a) Topology. (b) Idealized waveforms, gating signals can be found in [1].

condition iA (0) = −iA (π). This results in

$$i_A(0) = \frac{1}{3\omega L_s}\left[\frac{2\pi}{3}(V_o' - V_i) - V_o'\phi\right] \quad \text{.....(1)}$$

B. Output Power

Under the assumption of a lossless converter, the output power Po can be found with

$$P_o = P_i = \frac{3}{\pi}\int_0^{\pi} v_{AP}(\theta) i_A(\theta) d\theta. \qquad (2)$$

Finally, the expression of the output power for $0 \le \varphi \le 2\pi$ 3 is

C. Soft-Switching Region

Minimizing the switching losses is the key to achieve a high switching frequency. The turn-on losses are of main interest because excessive losses in the switch and the anti parallel diode can arise when the anti parallel

diodes experience the reverse recovery process. The input bridge faces this problem when iA (0) > 0. Therefore, the current has to ful fill iA (0) ≤ 0 to ensure soft-switching in the input bridge. During the switching transient, the current iA is considered constant. Rewriting (1) to the required constraint gives the phase shift for ensuring soft turn-on of the switches in the input bridge, this is found to be

$$\phi_{\mathrm{i}} \geq \frac{2\pi(V_{\mathrm{o}}' - V_{\mathrm{i}})}{3V_{\mathrm{o}}'}. \quad \text{.....(3)}$$

A similar derivation can be made for the output bridge, where the output bridge is soft-switching for iA (φ) ≥ 0. Using (3) and (1) gives the required phase shift to ensure soft turn-on of the switches in the output bridge, resulting in

$$\phi_{\mathrm{o}} \geq \frac{2\pi(V_{\mathrm{i}} - V_{\mathrm{o}}')}{3V_{\mathrm{i}}}. \quad \text{.....(4)}$$

1) Impact of ZVS Capacitors: ZVS capacitors, or snubber capacitors, are used to reduce turn-off losses. These are connected in parallel to the switches and supplement the output capacitance, as can be seen in Fig. 2(a). After a switch turns OFF, there is a small blanking time tb before the opposite switch of the same leg turns on. During tb , the current commutates to the ZVS capacitors and divides equally over the two capacitors of the phase leg. In this transition, one capacitor is charged while the other is discharged. This implies that the load current must be high enough to enable a full charge or discharge of the ZVS capacitors for a given tb . Assuming a constant current during the switching transient, the soft-switching constraint for enabling soft turn-on of the switches in the input bridge is changed to

$$i_{\mathrm{A}}(0) + \frac{2C_{\mathrm{s}}V_{i}}{t_{\mathrm{b}}} \leq 0 \quad \text{.....(5)}$$

and for the output bridge to

$$i_{\mathrm{A}}(\phi) - \frac{2C_{\mathrm{s}}V_{\mathrm{o}}}{t_{\mathrm{b}}N} \geq 0 \quad \text{.....(6)}$$

where Cs represents a ZVS capacitor connected in parallel to the switch, and tb is a fixed blanking time. A more accurate, current depending charge-based ZVS analysis is reported in [20]. However, to investigate the impact of the ZVS capacitors and approximate the soft-switching region, the presented current based method is sufficient.

Solving (7) and (8) for the phase-shift φ gives the soft switching region for the input bridge and the output bridge, respectively. These are given by

$$\phi_{\mathrm{i}} \geq \frac{2\pi_{i}(V_{\mathrm{o}}' - V_{\mathrm{i}})}{3V_{\mathrm{o}}'} + \frac{2C_{\mathrm{s}}V_{\mathrm{i}}}{V_{\mathrm{o}}'t_{\mathrm{b}}}3\omega L_{\mathrm{s}} \quad \text{.....(7)}$$

And

$$\phi_o \geq \frac{2\pi(V_i - V_o')}{3V_i} + \frac{2C_s V_o}{V_i t_b N} 3\omega L_s. \quad \text{.....(8)}$$

When satisfying both (9) and (10), a soft-switching region can be defined as function of the input voltage Vi, as shown in Fig. 3(a). The input voltage varies from 500 to 900V, which is given in Table I for light rail vehicles with a nominal voltage of 750 V. The reflected output voltage V o is chosen to equal the nominal input voltage of 750V to have a good utilization of the soft-switching region. Furthermore, the blanking time is chosen to be 10% of the switching cycle that means a duration of 5 μs

The soft-switching region can also be presented as the minimum output power versus the input voltage. An example is presented in Fig. 3(b) with the leakage inductance Ls set to 20 μH.

Fig. 3(a) and (b) shows that the ZVS capacitors decrease the soft-switching region. Especially, Fig. 3(b) shows the limitations for low- and high-input voltages. Therefore, the next section describes two methods to extend the soft-switching region.

D. Extension of the Soft-Switching Region

Auxiliary power converters for railway applications have to be able to operate from no-load to full-load conditions over the whole input voltage range. This means that the converter has to operate outside the soft-switching region. Therefore, two methods to extend the soft-switching operation of the converter have been investigated.

1) Auxiliary Inductors:

The first method is based on adding reactive currents to fully charge or discharge the ZVS capacitors during the switching transient. The reactive currents are injected with three star-connected auxiliary inductors per bridge, as can be seen in Fig. 4(a). This has the same effect as the magnetizing inductances of the transformers, which are also connected in star [23]. However, separate auxiliary inductors are preferred to have more design flexibility

The peak current, injected by the auxiliary inductors during the switching transient, is calculated from the voltage waveforms shown in Fig. 2(b). For the input bridge, the peak current is calculated as

$$\hat{i}_{a-i} = \frac{2\pi V_i}{9\omega L_{a-i}} \quad \text{.....(9)}$$

and for the output bridge as

$$\hat{i}_{a-o} = \frac{2\pi V_o}{9\omega L_{a-o} N}. \quad \text{.....(10)}$$

Next, the soft-switching constraints from (7) and (8) can be extended to

$$i_{\mathrm{A}}(0)+\frac{2C_{\mathrm{s}}V_{\mathrm{i}}}{t_{\mathrm{b}}}-\frac{2\pi V_{\mathrm{i}}}{9\omega L_{\mathrm{a-i}}}\leq 0 \quad \text{.....(11)}$$

and for the output bridge to

$$i_{\mathrm{A}}(\phi)-\frac{2C_{\mathrm{s}}V_{\mathrm{o}}}{t_{\mathrm{b}}N}+\frac{2\pi V_{\mathrm{o}}}{9\omega L_{\mathrm{a-o}}N}\geq 0. \quad \text{.....(12)}$$

Then, the soft-switching region can be calculated with the minimum phase shift for the input bridge

$$\phi_{\mathrm{i}}\geq\frac{2\pi(V_{\mathrm{o}}'-V_{\mathrm{i}})}{3V_{\mathrm{o}}'}+\frac{2C_{\mathrm{s}}V_{\mathrm{i}}}{V_{\mathrm{o}}'t_{\mathrm{b}}}3\omega L_{\mathrm{s}}-\frac{2\pi V_{\mathrm{i}}L_{\mathrm{s}}}{3V_{\mathrm{o}}'L_{\mathrm{a-i}}} \quad \text{....(13)}$$

and for the output bridge

$$\phi_{\mathrm{o}}\geq\frac{2\pi(V_{\mathrm{i}}-V_{\mathrm{o}}')}{3V_{\mathrm{i}}}+\frac{2C_{\mathrm{s}}V_{\mathrm{o}}}{V_{\mathrm{i}}t_{\mathrm{b}}N}3\omega L_{\mathrm{s}}-\frac{2\pi V_{\mathrm{o}}L_{\mathrm{s}}}{3V_{\mathrm{i}}L_{\mathrm{a-o}}N} \quad \text{.....(14)}$$

As shown with (15) and (16), the auxiliary inductance decreases the required phase-shift for operating in a soft-switching manner. To achieve soft-switching in the whole operating range, (15) and (16) should be solved for zero phase-shift, i.e., no-load condition. The corresponding values are shown in Fig. 4(b). For relatively low- and high-input voltages, the required values for La−i and La−o are low and, therefore, also causing high reactive currents. The use of auxiliary inductors presents a clear disadvantage due to the reduced efficiency and power density.

$$<p_{\mathrm{o}}>=\frac{n}{m}P_{\mathrm{b}},\qquad\forall\quad 1\leq n\leq m \quad \text{.....(15)}$$

where n is the amount of switching cycles operating with po = Pb and m is the total amount of switching cycles of one burst cycle. The value of Pb depends on the soft-switching region of the converter, an example is given in Fig. 3(b).

When nTs < t ≤ mTs, the output power po =0W, thus the output capacitor delivers the required current to the load, introducing a small voltage ripple. The output voltage ripple can be calculated with

$$\Delta v_{\mathrm{o}}=\frac{I_{\mathrm{o}}\Delta t}{C_{\mathrm{o}}} \quad \text{.....(16)}$$

where Io = Vo = nPb mVo and Δt = m−n fs . This results in

$$\Delta v_{\mathrm{o}}=\frac{n(m-n)P_{\mathrm{b}}}{mV_{\mathrm{o}}C_{\mathrm{o}}f_{\mathrm{s}}}. \quad \text{.....(17)}$$

An example of the output voltage ripple with n ≥ 2 is shown in Fig. 5(b).

IV-SIMULATION MODELLING AND DESIGN

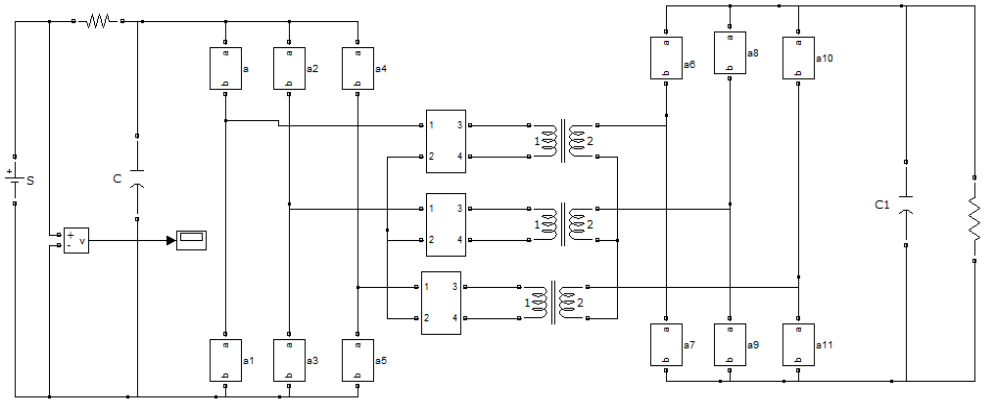

Fig:3. simulation modelling of proposed topology with dual active bridge

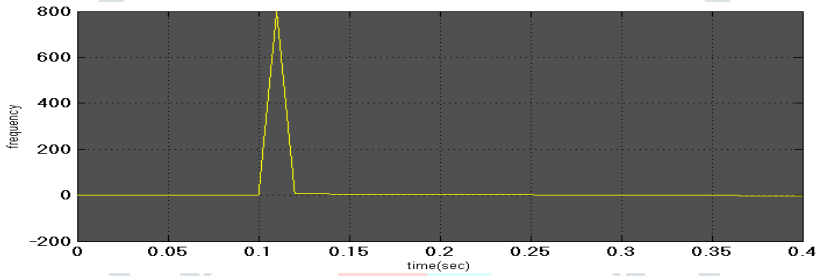

FIG:4.Turn-off switching transients, with Ic = 100 A, Vce = 800 V, (left) Cs = 0nF and (right) Cs = 110 nF.

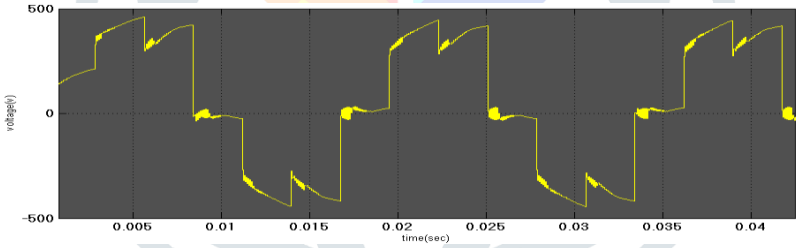

FIG:5.Measured converter waveform. (a) Vi = 500 V (100 V/div, 100 A/div, 10 µs/div),

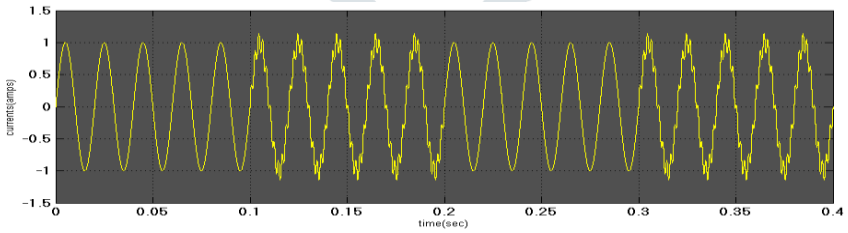

(A)

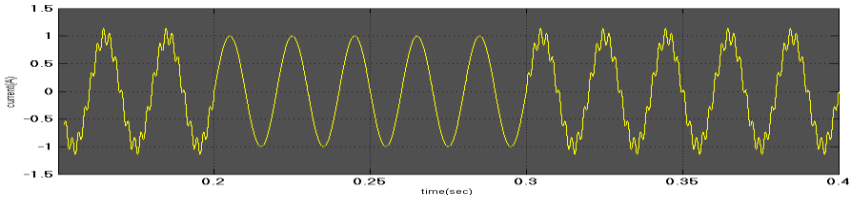

(B)

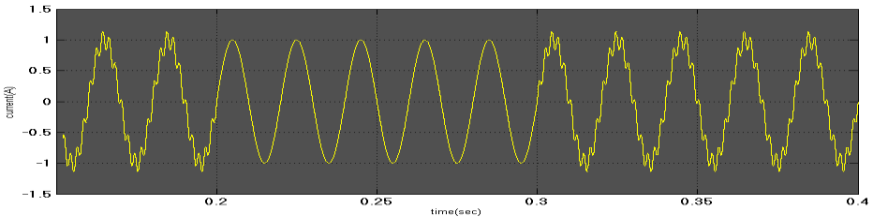

(C)

Phase currents during burst mode with m = 4, n = 2, Vi = 900 V, Co = 1 mF, Pb = 80 kW and Po = 40 kW (200 A/div, 50 μs/div).

V. CONCLUSION

The three-phase DAB topology has been selected for application in the APU because of the preferred properties concerning buck–boost operation, low device stress, small filters, high transformer utilization and low-switching losses. Subsequently, the soft-switching region is analyzed, including the effect of ZVS capacitors. Furthermore, two methods are presented to extend the soft-switching region: auxiliary inductors and a burst-mode switching strategy. Comprising a combination of the burst mode and auxiliary inductors, optimal component values are calculated to minimize the losses. As a result of the analysis, it is found that auxiliary inductors are not necessary with the use of the burst mode. Experimental results show good agreement of measured waveforms with the idealized model. Furthermore, efficiencies of the burst and continuous mode with a measured efficiency of 95.6% at maximum output power at nominal conditions are presented. Also, the use of ZVS capacitors shows about 40% reduction of the total loss, enabling an output power above nominal and still preserving a good efficiency. The prototype was tested thoroughly in the entire operating range, including operation in the burst mode with an input voltage of 500 and 900V. The burst mode proves to be useful to extend the operating range in a soft-switching manner. Operation during burst mode shows slightly lower efficiencies compared to continuous operation.

ACKNOWLEDGMENT

The authors would like to thank Strukton Rolling Stock, in particular J.Verschoor and W. Platschorre, for their support.

REFERENCES

[1] R. De Doncker, D. Divan, and M. Kheraluwala, "A three-phase soft switched high-power-density dc/dc converter for high-power applications," IEEE Trans. Ind. Appl., vol. 27, no. 1, pp. 63–73, Jan. 1991.

[2] J. Dudrik, P. Spanik, and N.-D. Trip, "Zero-voltage and zero-current switching full-bridge dc-dc converter with auxiliary transformer," IEEE Trans. Power Electron., vol. 21, no. 5, pp. 1328–1335, Sep. 2006.

[3] J.-G. Cho,C.-Y. Jeong, and F. Lee, "Zero-voltage and zero-current switching full-bridge PWM converter using secondary active clamp," IEEE Trans. Power Electron., vol. 13, no. 4, pp. 601–607, Jul. 1998.

[4] O. Patterson and D. Divan, "Pseudo-resonant full bridge dc/dc converter," IEEE Trans. Power Electron., vol. 6, no. 4, pp. 671–678, Oct. 1991.

[5] R. Steigerwald, "A comparison of half-bridge resonant converter topologies," IEEE Trans. Power Electron., vol. 3, no. 2, pp. 174–182, Apr. 1988.

[6] A. Bhat and R. Zheng, "Analysis and design of a three-phase LCC-type resonant converter," IEEE Trans. Aerospace and Electron. Syst., vol. 34, no. 2, pp. 508–519, Apr. 1998.

[7] R. Steigerwald, "High-frequency resonant transistor dc-dc converters," IEEE Trans. Ind. Electron., vol. IE-31, no. 2, pp. 181–191, May 1984.

[8] X. Li, "A LLC-type dual-bridge resonant converter: Analysis, design, simulation, and experimental results," IEEE Trans. Power Electron., vol. 29, no. 8, pp. 4313–4321, Aug. 2014.

[9] J.-W. Kim and G.-W. Moon, "A new LLC series resonant converter with a narrow switching frequency variation and reduced conduction losses," IEEE Trans. Power Electron., vol. 29, no. 8, pp. 4278–4287, Aug. 2014.

[10] S. De Simone, C. Adragna, C. Spini, and G. Gattavari, "Design-oriented steady-state analysis of LLC resonant converters based on FHA," in Proc. Int. Symp. Power Electron., Electr. Drives, Autom. Motion,, May 2006, pp. 200–207.